

Internal lipid bilayer friction coefficient from equilibrium canonical simulations

Othmene Benazieb,¹ Lisa Berezovska,¹ and Fabrice Thalmann¹

¹*Institut Charles Sadron, CNRS and University of Strasbourg,
23 rue du Loess, F-67034 Strasbourg cedex 2, France*

(Dated: May 9, 2022)

A fundamental result in the theory of Brownian motion is the Einstein-Sutherland relation between mobility and diffusion constant. Any classical linear response transport coefficient obeys a similar Einstein-Helfand relation. We show in this work how to derive the interleaflet friction coefficient of lipid bilayer by means of an adequate generalisation of the Einstein relation. Special attention must be paid in practical cases to the constraints on the system center of mass position that must be enforced when coupling the system to thermostat.

In 1905 Einstein [1] and Sutherland [2] obtained a relation $D = k_B T \nu$ between the diffusion coefficient D of a Brownian particle, its mobility coefficient ν (ratio between average drift velocity and drift force) the absolute temperature T and the Boltzmann constant k_B . Similar relations were later established for all the usual transport coefficients (viscosity, thermal conduction, . . .), the Einstein-Helfand relations [3]. These expressions provide an alternative way to the Green-Kubo relations for the determination of the transport properties, based on the averaged mean square deviation (MSD) of well chosen dynamical observables. The use of Helfand expressions in molecular dynamics (MD) simulation is however not always practical due to system periodic boundary conditions (PBC) [4, 5].

A natural question arises as to determining lipid bilayer friction properties in a similar way, *i.e.* by writing and computing the MSD of a carefully chosen dynamical observable. Such result would be valuable as an alternative to out-of-equilibrium simulation techniques, which are diversely implemented in the commonly used simulation packages.

A model bilayer system comprising two apposed leaflets and a single water solvent slab is expected (Fig. 1) to maintain its self-assembled structure for the longest available simulation times. Two-tails standard lipid molecules are too little soluble in water [6, 7] to escape from the bilayer, and have very long leaflet exchange characteristic times [8, 9]. Therefore the only molecular motions expected in such a case are the in-plane self diffusion of lipid molecules and bulk diffusion of water molecules. Let us then decompose the system into three apposed subsystems: upper lipid leaflet (S_1), lower lipid leaflet (S_2) and solvent (S_3). Denoting x_i the respective horizontal coordinates of the subsystems, one faces the problem of finding a relation between the average displacements covariance matrix $D_{ij}(t) = \langle (x_i(t) - x_j(0))^2 \rangle$, $i, j = 1, 2, 3$, with brackets $\langle \cdot \rangle$ standing for the canonical equilibrium trajectories average, and the desired friction coefficients.

Simulated molecular systems must be coupled to thermostats to generate representative canonical trajectories

and keep the system internal energy constant. A number of popular momentum preserving thermostat such as Nose-Hoover chains or V-rescale thermostat requires in turn that the center of mass of the system remains fixed to some arbitrary position, and that no external finite force is applied to the system (mechanical insulation) [10–13]. In what follows, we adopt this convention throughout.

The continuous hydrodynamic description of a lipid bilayer system consists in replacing each leaflet by a solid thick slab, and water by a fluid slab at fixed vertical positions (Fig. 1). This assumes a low water permeability of the membrane on the one hand (verified in practice) and a system center of mass fixed. We assume xy planar isotropy and restrict ourselves to the x component of the displacements. The hydrodynamic system is characterized by two masses $m_1 = m_2 = m$ and two velocity scalars V_1, V_2 associated to the leaflets, along with a mass density ρ and a continuous velocity field $v_x(z)$ for the water slab. The water mass m_w and center of mass velocity V_w follow from integrating ρ and $v_x(z)$ along z . The solvent flow is assumed to be linear parabolic at all times, a situation covering the Couette and Poiseuille velocity profiles. In the absence of sliding, the flow is completely parametrized by V_1, V_2 and V_w , considered as the slow variables of the many particles system. When connecting these hydrodynamic variables to molecular simulations, it is necessary to account for possible PBC jumps in the molecular displacements, and to consider continuous, unwrapped trajectories. Subsystems are possibly acted upon by forces F_1, F_2, F_3 in the x direction. Mechanical insulation requires $F_1 + F_2 + F_3 = 0$ while the stationary system center of mass imposes $m_1 V_1 + m_2 V_2 + m_3 V_3 = 0$. As explained in [14], the equations of motions of the 3 subsystems read, in the absence of water-lipid bilayer sliding,

$$\begin{aligned} m_1 \dot{V}_1 &= \left(bA - \frac{2\eta A}{L_w} \right) (V_2 - V_1) + \frac{6\eta A}{L_w} (V_3 - V_1) + F_1; \\ m_2 \dot{V}_2 &= \left(bA - \frac{2\eta A}{L_w} \right) (V_1 - V_2) + \frac{6\eta A}{L_w} (V_3 - V_2) + F_2; \\ m_3 \dot{V}_3 &= \frac{6\eta A}{L_w} (V_1 + V_2 - 2V_3) + F_3, \end{aligned} \quad (1)$$

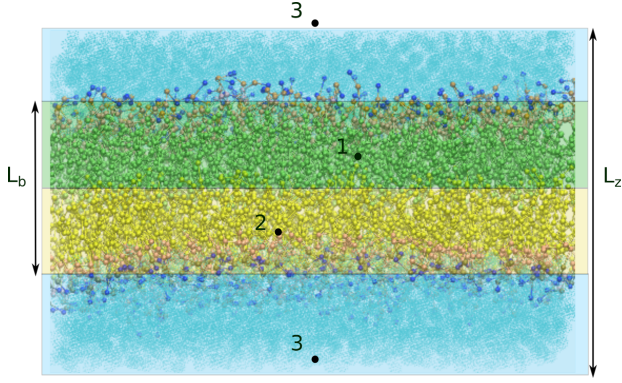


FIG. 1. Coarse-Grained MD snapshot superimposed with the two solid blocks (1,2) and water solvent (3). Each of the 3 components is uniquely located by a single center of mass coordinate along the x direction. The solvent flow is linear-parabolic in the z direction, L_z is the thickness of the (periodic) box, L_b the bilayer thickness, $L_w = L_z - L_b$ the water thickness.

where A is the area of the slab, η the Newtonian viscosity of the solvent and b the interleaflet friction coefficient. The relation expresses that internal forces between components are proportional to the system area, and linearly dependent on the mutual velocity differences.

The purpose of the Letter is to establish an Einstein-Helfand relation for the frictions coefficients b and η/L_w . For this purpose we generalize the Langevin-Smoluchovski (overdamped) stochastic equation of motion $d(mv) = -\zeta v dt + \sqrt{2m\zeta k_B T} dW(t)$ of a Brownian particle (m mass, v velocity, ζ "Stokes"-friction coefficient, t time, dW differential of a normalized Wiener process) [15]. It is well known in this situation that the Brownian diffusion coefficient equals $k_B T/\zeta$ and that the average kinetic energy $mv^2/2 = k_B T/2$ is given by the equipartition theorem. The generalization in the case of the 3 slabs reads:

$$d\mathbf{p} = -A\mathbf{p}dt + B d\mathbf{W}(t), \quad (2)$$

$\mathbf{p} = (mV_1, mV_2, m_w V_3)$ being a vector of impulsions and $\mathbf{W}(t)$ 3 independent normalized Wiener processes. The mass \mathcal{M} and friction \mathcal{A} matrices follow from eq. 1.

$$\begin{aligned} \mathcal{M} &= \begin{pmatrix} m & 0 & 0 \\ 0 & m & 0 \\ 0 & 0 & m_w \end{pmatrix} = \mathcal{M}^T; \\ \mathcal{A}\mathcal{M} &= A \begin{pmatrix} b + 4\eta/L_w & -b + 2\eta/L_w & -6\eta/L_w \\ -b + 2\eta/L_w & b + 4\eta/L_w & -6\eta/L_w \\ -6\eta/L_w & -6\eta/L_w & 12\eta/L_w \end{pmatrix} \\ &= \mathcal{M}\mathcal{A}^T. \end{aligned} \quad (3)$$

The mass matrix relates the velocities vector $\mathbf{v} = (V_1, V_2, V_3)$ to the impulsions $\mathbf{p} = \mathcal{M}\mathbf{v}$. The random noise matrix \mathcal{B} (defined up to a $\mathcal{O}(3)$ orthogonal transformation) must be chosen so that the correct canonical average $\langle \mathbf{p}\mathbf{p}^T \rangle$ is recovered, \mathbb{T} representing the real transpose of vectors and matrices. This implies [15]

$$A \cdot \langle \mathbf{p}\mathbf{p}^T \rangle + \langle \mathbf{p}\mathbf{p}^T \rangle \cdot A^T = \mathcal{B}\mathcal{B}^T. \quad (5)$$

However, due to the use of a thermostat, a momentum conservation constraint $\mathbf{U}^T \mathbf{p} = 0$ holds, with $\mathbf{U} = (1, 1, 1)$. The friction matrix \mathcal{A} is only of rank 2 as $\mathbf{U}^T \mathcal{A} = 0$ (so does $\mathcal{A}\mathcal{M}\mathbf{U} = 0$).

The total vanishing impulsion constraint modifies the energy equipartition theorem, as the thermal energy $k_B T$ of two degrees of freedom is shared by the three subsystems according to their respective inverse masses. A calculation (Supplemental Material, SM) gives

$$\langle \mathbf{v}\mathbf{v}^T \rangle = k_B T \left[\mathcal{M}^{-1} - \frac{\mathbf{U}\mathbf{U}^T}{m_t} \right], \quad (6)$$

with $m_t = m_1 + m_2 + m_3$ the total mass. The impulsion covariance matrix follows immediately, given $\mathcal{M}^T = \mathcal{M}$:

$$\langle \mathbf{p}\mathbf{p}^T \rangle = \mathcal{M}^T \langle \mathbf{v}\mathbf{v}^T \rangle \mathcal{M} = k_B T \left[\mathcal{M} - \mathcal{M} \frac{(\mathbf{U}\mathbf{U}^T)}{m_t} \mathcal{M} \right].$$

Combining eqs. 5 and 7 along with the constraints $\mathcal{A}\mathcal{M}\mathbf{U} = 0$ and $\mathbf{U}^T \mathcal{M}\mathcal{A}^T = 0$ leads to a simple expression for the random force correlations

$$\mathcal{B}\mathcal{B}^T = k_B T (\mathcal{A}\mathcal{M} + \mathcal{M}\mathcal{A}^T) = 2k_B T \mathcal{A}\mathcal{M}. \quad (7)$$

Meanwhile, the long times (damped) displacement covariance matrix can be obtained by integrating eq. 2, leading to a displacement vector $\Delta \mathbf{x} = (x_i(t) - x_i(0))$ in terms of the vector of Wiener processes ($W_i(t)$), given by $\mathcal{A}\mathcal{M}\Delta \mathbf{x}(t) = \mathcal{B}\mathbf{W}(t)$ and thus $\mathcal{A}\mathcal{M}\Delta \mathbf{x}\Delta \mathbf{x}^T (\mathcal{A}\mathcal{M})^T = \mathcal{B}\mathbf{W}\mathbf{W}^T \mathcal{B}^T$. Taking the thermal average leads to

$$\mathcal{A}\mathcal{M}\langle \Delta \mathbf{x}\Delta \mathbf{x}^T \rangle \mathcal{A}\mathcal{M} = \mathcal{B}\mathcal{B}^T t = 2k_B T \mathcal{A}\mathcal{M} t. \quad (8)$$

Eq. 8 formally solves the problem, by connecting the covariance displacement matrix on the left hand side with the friction matrix $\mathcal{A}\mathcal{M}$ on the right hand side. It represents the desired Einstein-Helfand expression for the lipid bilayer frictions. Nevertheless, the expression is not useful as such, due to $\mathcal{A}\mathcal{M}$ being a rank 2 matrix. It cannot be explicitly inverted to yield the desired displacement covariance matrix alone on the left hand side of an equation. Eq. 8 takes actually a Moore-Penrose pseudo-inverse matrix form.

In the case of interest, it is possible to express the covariance matrix using the orthogonal change of basis

$$O = \frac{1}{\sqrt{3}} \begin{pmatrix} \frac{1+\sqrt{3}}{2} & \frac{1-\sqrt{3}}{2} & 1 \\ \frac{1-\sqrt{3}}{2} & \frac{1+\sqrt{3}}{2} & 1 \\ -1 & -1 & 1 \end{pmatrix}; \quad O^T \mathcal{A} \mathcal{M} O = A \begin{pmatrix} b + \frac{10\eta}{L_w} & \frac{8\eta}{L_w} - b & 0 \\ \frac{8\eta}{L_w} - b & b + \frac{10\eta}{L_w} & 0 \\ 0 & 0 & 0 \end{pmatrix}. \quad (9)$$

Parameterizing the displacement covariance matrix \mathcal{D} with Voigt indices 4,5,6, $D_1 = D_2$ and $D_4 = D_5$

$$\begin{pmatrix} \langle (\Delta \mathbf{x}_1)^2 \rangle & \langle \Delta \mathbf{x}_1 \Delta \mathbf{x}_2 \rangle & \langle \Delta \mathbf{x}_1 \Delta \mathbf{x}_3 \rangle \\ \langle \Delta \mathbf{x}_2 \Delta \mathbf{x}_1 \rangle & \langle (\Delta \mathbf{x}_2)^2 \rangle & \langle \Delta \mathbf{x}_2 \Delta \mathbf{x}_3 \rangle \\ \langle \Delta \mathbf{x}_3 \Delta \mathbf{x}_1 \rangle & \langle \Delta \mathbf{x}_2 \Delta \mathbf{x}_3 \rangle & \langle (\Delta \mathbf{x}_3)^2 \rangle \end{pmatrix} = 2 \begin{pmatrix} D_1 & D_6 & D_4 \\ D_6 & D_1 & D_4 \\ D_4 & D_4 & D_3 \end{pmatrix} t, \quad (10)$$

leads to the explicit inverse relation

$$\frac{3k_B T}{A} \begin{pmatrix} 1 & 0 \\ 0 & 1 \end{pmatrix} = \begin{pmatrix} b + \frac{10\eta}{L_w} & \frac{8\eta}{L_w} - b \\ \frac{8\eta}{L_w} - b & b + \frac{10\eta}{L_w} \end{pmatrix} \cdot \begin{pmatrix} (2D_1 - D_6 + D_3 - 2D_4) & (2D_6 - D_1 + D_3 - 2D_4) \\ (2D_6 - D_1 + D_3 - 2D_4) & (2D_1 - D_6 + D_3 - 2D_4) \end{pmatrix}. \quad (11)$$

Equation 11 is a 2×2 matrix generalization of the Stokes-Einstein relation, and constitutes the main result of this Letter. It is easy to establish two further relations between the covariance parameters

$$m_w D_3 + 2m D_4 = 0; \quad m(D_1 + D_6) + m_w D_4 = 0, \quad (12)$$

showing that only two independent degrees of freedom are left in the displacement covariance matrix to match the two independent degrees of freedom of the friction matrix b and η/L_w . Eq. 12 follows from the time integration of $\mathbf{v} \mathcal{M} \mathbf{U} = 0$, proving that the displacement vector $\Delta \mathbf{x}(t)$ stays always orthogonal to $\mathcal{M} \mathbf{U}$. Note that the presentation of eq. 11 is not unique, due to a $O(1)$ degeneracy associated with the choice of the orthogonal matrix O , whose sole effect is to rotate the 2 coordinates in 11.

We now check that the Brownian description proposed predicts correctly the behavior of a simulated lipid membrane system (coarse-grained Martini model [16], 512 lipids, 10 μs simulated, see SM for details). Predictions for the velocity covariance matrix can be assessed by estimating the deviation ε_{ept} from the expected result, using the matrix norm $\|X\|_q^2 = \text{tr}(X X^T)$ (see eq 7):

$$\varepsilon_{\text{ept}} = \left\| k_B T \left[\mathcal{M}^{-1} - \frac{\mathbf{U} \mathbf{U}^T}{m_t} \right] - \langle \mathbf{v} \mathbf{v}^T \rangle \right\|_q / \left\| \langle \mathbf{v} \mathbf{v}^T \rangle \right\|_q. \quad (13)$$

We find good agreement with the prediction as $\varepsilon_{\text{ept}} \simeq 1.8 \times 10^{-3}$ is of the order of two parts per thousand. Using the same data and the Einstein-Helfand relation (11) we obtained respectively $b = 2.54 \times 10^6 \text{ Pa s m}^{-1}$ and $\eta = 8.1 \times 10^{-4} \text{ Pa s}$, with an estimated relative accuracy of the order of 0.05 (see SM). This compares favorably with the reported values, for the same system and conditions, of $b = 2.55 \pm 0.10 \times 10^6 \text{ Pa s m}^{-1}$ and $\eta = 8. \times 10^{-4} \text{ Pa s}$ [14].

We have so far shown how the standard Wiener process for damped Brownian motion generalizes to the case of constrained vanishing total momentum. In doing so, one finds eq. 8 as the generalization of the

2^{nd} fluctuation-dissipation theorem. A natural question arises as whether it is possible to write an equivalent version of the 1^{st} fluctuation-dissipation theorem (FDT), which relates the linear response of a system to an equilibrium correlation function. The unbounded free Brownian motion is unfortunately not an equilibrium situation, with the 1st FDT violated [17]. It is therefore necessary to place the system under conditions consistent with a stationary thermal equilibrium state. The harmonic confinement potential is the simplest and most natural example. Once the FDT proven in the harmonic case, it can in principle be extended perturbatively to nonlinear analytic potentials [18, 19].

For this purpose, we now consider the damped Brownian (Smoluchowski) process (2) in the presence of a linear force field

$$\mathcal{A} \mathcal{M} d\mathbf{x} + \mathcal{K} \mathbf{x} dt = \mathcal{B} d\mathbf{W}(t) + \mathbf{f}(t) dt \quad (14)$$

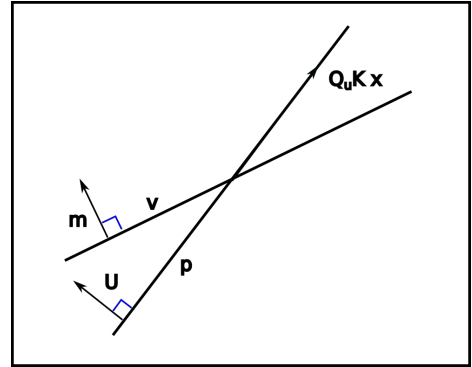


FIG. 2. Illustration of the projection procedure. Velocities are constrained to an hyperplane $\mathbf{m}^T \mathbf{v} = 0$, momenta are constrained to the hyperplane $\mathbf{U}^T \mathbf{p} = 0$. To satisfy the conservation of the center of mass position, the linear force $\mathcal{K} \mathbf{x}$ must be projected onto the momenta hyperplane. In simulations, the constraint on the system center of mass position acts by removing the out-of-plane component of the force.

with $\mathbf{x} = (x_1(t), x_2(t), x_3(t))$ the stochastic trajectory, $\mathbf{p} = \mathcal{M}\mathbf{x}$, $\mathcal{K} = \mathcal{K}_{ij}$ a symmetric curvature matrix representing the linear conservative force-field and $\mathbf{f}(t)$ the arbitrary time dependent external force conjugated to the average position response $\langle \mathbf{x}(t') \rangle$ at posterior times $t' > t$. The harmonic and perturbation forces must both be consistent with a total vanishing (conserved total momentum) constraint $\mathbf{U}^\top \mathcal{K} = \mathcal{K}\mathbf{U} = 0$ and $\mathbf{U}^\top \mathbf{f}(t) = 0$. The motion is restricted to the orthogonal subspace $U^\top \mathcal{M}\mathbf{x} = 0$, denoted m^\perp , while all forces and momenta belongs the orthogonal subspace U^\perp . Positiveness of the harmonic potential requires $\mathbf{x}^\top \mathcal{K}\mathbf{x} > 0$. The problem reduces to computing the correlation and response properties of the projected vector $\mathcal{Q}_u \mathbf{x}(t)$ orthogonal to \mathbf{U} , with $\mathcal{Q}_u = \mathbb{1} - \mathbf{U}\mathbf{U}^\top/3$ (Figure 2). Expressing the original displacement \mathbf{x} in terms of the projected $\mathcal{Q}_u \mathbf{x}(t)$ is straightforward:

$$\mathbf{x} = \left(\mathbb{1} - \frac{\mathbf{U}\mathbf{m}^\top}{m_t} \right) \mathcal{Q}_u \mathbf{x}. \quad (15)$$

Let us now determine the statistical properties of $\mathcal{Q}_u \mathbf{x}$. We first observe that $\mathcal{Q}_u \mathcal{A}\mathcal{M}\mathcal{Q}_u = \mathcal{A}\mathcal{M}$ and $\mathcal{K}\mathcal{Q}_u = \mathcal{K}$.

Eq. 14 can be rewritten as

$$\mathcal{Q}_u \mathcal{A}\mathcal{M}\mathcal{Q}_u \mathcal{Q}_u d\mathbf{x} + \mathcal{K}\mathcal{Q}_u \mathbf{x} dt = \mathcal{B}d\mathbf{W}(t) + \mathbf{f}(t)dt. \quad (16)$$

The projected dissipation matrix $\mathcal{Q}_u \mathcal{A}\mathcal{M}\mathcal{Q}_u$ is invertible in the vector subspace U^\perp orthogonal to \mathbf{U} , and its rank 2 inverse denoted $\mathcal{J}_u = \{\mathcal{Q}_u \mathcal{A}\mathcal{M}\mathcal{Q}_u\}^{-1}$. All terms in 16 belong to U^\perp . The projected stochastic solution reads

$$\begin{aligned} \mathcal{Q}_u \mathbf{x}(t) = & \exp(-\mathcal{J}_u \mathcal{K}t) \mathcal{Q}_u \mathbf{x}(0) + \\ & + \int_0^t \exp(-\mathcal{J}_u \mathcal{K}(t-s)) \mathcal{J}_u [\mathcal{B}d\mathbf{W}(s) + \mathbf{f}(s)ds], \end{aligned} \quad (17)$$

from which the undriven $\mathbf{f} = 0$ correlation for $t > 0$

$$\begin{aligned} \mathcal{C}_u(t) = & \langle \mathcal{Q}_u \mathbf{x}(t) \mathbf{x}(0)^\top \mathcal{Q}_u \rangle \\ = & \exp(-\mathcal{J}_u \mathcal{K}t) \langle \mathcal{Q}_u \mathbf{x}(0) \mathbf{x}(0)^\top \mathcal{Q}_u \rangle \end{aligned} \quad (18)$$

and the causal response $\mathcal{R}_u(t) = \exp(-\mathcal{J}_u \mathcal{K}t) \mathcal{J}_u$, defined by $\delta \langle \mathcal{Q}_u \mathbf{x}(t) \rangle = \int_0^t \mathcal{R}_u(t-s) \delta \mathbf{f}(s) ds$ can be obtained. Similar reasoning as eq. 8 leads to a stationary covariance matrix

$$\lim_{t \rightarrow \infty} \langle \mathcal{Q}_u \mathbf{x}(t) \mathbf{x}(t)^\top \mathcal{Q}_u \rangle = \langle \mathcal{Q}_u \mathbf{x} \mathbf{x}^\top \mathcal{Q}_u \rangle_{st} = k_B T \{\mathcal{Q}_u \mathcal{K} \mathcal{Q}_u\}^{-1}, \quad (19)$$

ensuring energy equipartition into the two harmonic potential degrees of freedom. The stationary projected correlation function therefore simplifies as

$$\mathcal{C}_u(t) = \langle \mathcal{Q}_u \mathbf{x}(t) \mathbf{x}(0)^\top \mathcal{Q}_u \rangle = k_B T \{ H(t) \exp(-\mathcal{J}_u \mathcal{K}t) \{\mathcal{Q}_u \mathcal{K} \mathcal{Q}_u\}^{-1} + H(-t) \{\mathcal{Q}_u \mathcal{K} \mathcal{Q}_u\}^{-1} \exp(\mathcal{K} \mathcal{J}_u t) \} \quad (20)$$

where a Heaviside function $H(t)$ distinguishes positive and negative time values, and account for a possible non commutation of the $\mathcal{A}\mathcal{M}$ and \mathcal{K} matrices. It is then clear that, in this form, a first fluctuation dissipation theorem

$$\frac{d\mathcal{C}_u}{dt} = k_B T \{ H(t) \mathcal{R}_u(t) - H(-t) \mathcal{R}_u^\top(-t) \} \quad (21)$$

holds. Expressing the relation between $\mathcal{C}(t) = \langle \mathbf{x}(t) \mathbf{x}(0)^\top \rangle$ and $\mathcal{R}(t) = \delta \langle \mathbf{x}(t) \rangle / \delta \mathbf{f}(0)$ using 15 is immediate.

To conclude, we have introduced an original equilibrium fluctuation relation between the center of mass mutual diffusion coefficients of a simulated lipid membrane with periodic boundary conditions and the viscous dissipation coefficients (interleaflet friction and solvent viscosity) relevant to the motion in the bilayer plane. This result assumes that no lipid exchange takes place, and that solvent penetration into the membrane can be neglected. It is consistent with the use of a thermostat where the center of mass of the whole system is forced to be static. It is based on a macroscopic long range and long times hydrodynamic description of the mutual bilayer components displacements. It also disregards any

sliding of the solvent at the bilayer interface, usually considered as negligible as a first approximation. The diffusion parameters introduced in the discussion depends on the area of the simulated system, very much like the Stokes sphere mobility depends on its radius. A compromise must be found between increasing the system size to reach some hydrodynamic limit, and keeping it small enough to prevent Helfrich undulations [20] and preserving enough leaflet Brownian diffusion. With very little extra-cost in terms of simulation and analysis, this result is poised to become a standard characterization of realistic numerical membranes, provided they are simulated long enough for the leaflet center of mass displacements to be estimated.

Acknowledgement The authors would like to acknowledge the High Performance Computing Center of the University of Strasbourg for supporting this work by providing scientific support and access to computing resources (grant g2021a337c).

-
- [1] A. Einstein. Über die von der molekularkinetischen theorie der wärme geforderte bewegung von in ruhenden flüssigkeiten suspendierten teilchen. *Annalen der Physik*, 322(8):549–560, 1905.
- [2] W. Sutherland. A dynamical theory of diffusion for non electrolytes and the molecular mass of albumines. *Philosophical Magazine*, 9(54):781, 1905.
- [3] E. Helfand. Transport coefficients from dissipation in a canonical ensemble. *Phys. Rev.*, 119:1–9, Jul 1960.
- [4] S. Viscardy, J. Servantie, and P. Gaspard. Transport and helfand moments in the lennard-jones fluid. I. Shear viscosity. *J. Chem. Phys.*, 126(18):184512, 2007.
- [5] S. Viscardy, J. Servantie, and P. Gaspard. Transport and helfand moments in the lennard-jones fluid. II. Thermal conductivity. *J. Chem. Phys.*, 126(18):184513, 2007.
- [6] J. N Israelachvili. *Intermolecular and Surface Forces*. Elsevier, Oxford, 1992.
- [7] D. Fennell Evans and Wennerström Håkan. *The Colloidal Domain: Where Physics, Chemistry, Biology, and Technology Meet*. Wiley-VCH, New-York, 2nd edition, 1999.
- [8] H. M. McConnell and R. D. Kornberg. Inside-outside transitions of phospholipids in vesicle membranes. *Biochemistry*, 10(7):1111–1120, 1971.
- [9] L. A. Bagatolli and O. G. Mouritsen. *Life - As a Matter of Fat*. Springer-Verlag GmbH, Berlin, 2015.
- [10] W. G. Hoover. Generalization of nosé’s isothermal molecular dynamics: Non-hamiltonian dynamics for the canonical ensemble. *Phys. Rev. A*, 40:2814–2815, 1989.
- [11] G. Bussi, D. Donadio and M. Parrinello. Canonical sampling through velocity rescaling. *J. Chem. Phys.*, 126(1):014101, 2007.
- [12] D. Frenkel and B. Smit. *Understanding Molecular Simulations: From Algorithms to Applications*. Academic Press, San Diego, 2002.
- [13] M. E. Tuckerman. *Statistical Mechanics: Theory and Molecular Simulations*. Oxford University Press, Oxford, 1st edition, 2010.
- [14] O. Benazieb, C. Loison and F. Thalmann. Rheology of sliding leaflets in coarse-grained DSPC lipid bilayers. *Phys. Rev. E*, 104(5), nov 2021.
- [15] C. W. Gardiner. *Handbook of Stochastic Methods for Physics, Chemistry and the Natural Sciences*. Springer-Verlag, Berlin, 1985.
- [16] S. J. Marrink et al. The MARTINI Force Field: Coarse Grained Model for Biomolecular Simulations *J. Chem. Phys. B*, 111:7812, 2007
- [17] L. Cugliandolo, J. Kurchan and G. Parisi. Off equilibrium dynamics and aging in unfrustrated systems. *Journal de Physique I(France)*, 4(11):1641, 1994.
- [18] U. Decker and F. Haake. Fluctuation-dissipation theorems for classical processes. *Phys. Rev. A*, 11:2043–2056, 1975.
- [19] J. P. Bouchaud, L. Cugliandolo, J. Kurchan, and M. Mézard. Mode-coupling approximations, glass theory and disordered systems. *Physica A*, 226:243, 1996.
- [20] S. Safran. *Statistical Thermodynamics of Surfaces, Interfaces and Membranes*. Addison-Wesley, Reading, MA, 1994.
- [21] Zenodo repository of Gromacs initial configurations, topology, MD parameter files available at <https://doi.org/10.5281/zenodo.6514281>.

Internal lipid bilayer friction coefficient from equilibrium canonical simulations. Supplemental Material

Othmene Benazieb, Lisa Berezovska, Fabrice Thalmann
Institut Charles Sadron, CNRS and University of Strasbourg,
23 rue du Loess, F-67034 Strasbourg cedex 2, France

May 9, 2022

Simulation conditions

Our simulations are based on the Martini v2.0 lipid coarse-grained force field [1], and use 512 distearoylphosphatidylcholine (DSPC, 5 beads chain model) along with 5120 water bead molecules. The DSPC bilayer is numerically fluid at 340 K, simulated temperature.

The MD simulation engine was Gromacs 2018.4 [2]. After an initial equilibration stage, we let the system evolve in contact with a V-rescale thermostat (coupling time 1 ps) with separately coupled DSPC and water groups and a Parinello-Rahman semiisotropic barostat (coupling time 12 ps, compressibility $3 \times 10^{-4} \text{ bar}^{-1}$). The integration time step was $dt = 10 \text{ fs}$. A total of 25 consecutive trajectories of 400 ns each, cumulating to 10 μs were used in the statistics presented here. The 25 trajectories were used combined into a bootstrap statistical analysis of the variability of the presented results.

Trajectory file in Gromacs binary format `trr` were created recording center of forces positions and velocities every 20 ps. Home made C softwares based on Gromacs libraries were used to manipulate index and trajectory files, taking care of periodic boundary conditions jumps, computing observables such as leaflet and solvent center of mass positions and determining instantaneous kinetic energies. Mean squared displacements were computed from the subsystem center of mass trajectories.

Equipartition of energy

The system comprises three spatially separated components: the upper and lower leaflets and the water slab. Molecular exchange between components, for a phospholipid bilayer simulated under normal conditions of pressure and temperature, is marginal, corresponding mostly to water beads transits across bilayers. An instantaneous center of mass velocity can be defined. The canonical equilibrium distribution is supposed to be valid, which can be explicitly verified in our case, see eq 9.

For the sake of generality, we address first the situation with three arbitrary masses $\mathbf{m} = (m_1, m_2, m_3)$. In the Maxwell velocity distribution, the three euclidean directions are uncoupled, and it is sufficient to restrict ourselves the x component. This amounts to considering a center of mass velocity vector $\mathbf{v} = (V_1, V_2, V_3)$, subject to a kinematic constraint $\mathbf{m}^T \mathbf{v} = 0$.

The instantaneous center of mass velocity covariance matrix

$$\langle v_i v_j \rangle = \frac{\int d\mathbf{v} (v_i v_j) \delta(\mathbf{m}^T \mathbf{v}) \exp[-\frac{\beta}{2}(m_1 v_1^2 + m_2 v_2^2 + m_3 v_3^2)]}{\int d\mathbf{v} \delta(\mathbf{m}^T \mathbf{v}) \exp[-\frac{\beta}{2}(m_1 v_1^2 + m_2 v_2^2 + m_3 v_3^2)]} \quad (1)$$

can be computed in a number of different manners, all leading to the same result. It turns out that the computation of the impulsions covariance matrix is simpler.

$$\langle p_i p_j \rangle = \frac{\int d\mathbf{p} (p_i p_j) \delta(\mathbf{U}^\top \mathbf{p}) \exp[-\frac{\beta}{2}(\frac{p_1^2}{m_1} + \frac{p_2^2}{m_2} + \frac{p_3^2}{m_3})]}{\int d\mathbf{p} \delta(\mathbf{U}^\top \mathbf{p}) \exp[-\frac{\beta}{2}(\frac{p_1^2}{m_1} + \frac{p_2^2}{m_2} + \frac{p_3^2}{m_3})]} \quad (2)$$

One takes advantage of the mass matrix \mathcal{M} to express the kinetic energy $\mathbf{p}^\top \mathcal{M}^{-1} \mathbf{p} / 2$ and one uses the following gaussian regularization of the δ :

$$\delta(\mathbf{U}^\top \mathbf{p}) = \lim_{\varepsilon \downarrow 0} \frac{1}{\sqrt{2\pi\varepsilon}} e^{-\frac{\mathbf{p}^\top \mathbf{U} \mathbf{U}^\top \mathbf{p}}{2\varepsilon}} \quad (3)$$

A classical result on multidimensional gaussian integrals states that

$$\begin{aligned} \langle \mathbf{p} \mathbf{p}^\top \rangle &= \lim_{\varepsilon \downarrow 0} \left(\beta \mathcal{M}^{-1} + \frac{\mathbf{U} \mathbf{U}^\top}{\varepsilon} \right)^{-1} \\ &= \lim_{\varepsilon \downarrow 0} \varepsilon \left(\varepsilon \beta \mathcal{M}^{-1} + \mathbf{U} \mathbf{U}^\top \right)^{-1} \end{aligned} \quad (4)$$

Guessing for a matrix inverse form $C_1 \mathcal{M} + C_2 \mathbf{m} \mathbf{m}^\top$ with C_1, C_2 numerical constants to determine leads to

$$(\varepsilon \beta \mathcal{M}^{-1} + \mathbf{U} \mathbf{U}^\top)(C_1 \mathcal{M} + C_2 \mathbf{m} \mathbf{m}^\top) = (\varepsilon \beta C_1) \mathbb{1} + (C_1 + m_t C_2 + \varepsilon \beta C_2) \mathbf{U} \mathbf{m}^\top \quad (5)$$

with $m_t = \text{tr}(\mathcal{M})$ representing the total mass. This implies $\varepsilon \beta C_1 = 1$ and $C_1 + (m_t + \varepsilon \beta) C_2 = 0$. The matrix inverse is therefore equal to

$$\frac{1}{\beta \varepsilon} \left(\mathcal{M} - \frac{\mathbf{m} \mathbf{m}^\top}{m_t + \varepsilon \beta} \right) \quad (6)$$

Then finally in the $\varepsilon \rightarrow 0$ limit

$$\langle p_i p_j \rangle = k_B T \left(\mathcal{M} - \frac{\mathbf{m} \mathbf{m}^\top}{m_t} \right) \quad (7)$$

$$\langle v_i v_j \rangle = k_B T \left(\mathcal{M}^{-1} - \frac{\mathbf{U} \mathbf{U}^\top}{m_t} \right) \quad (8)$$

This result is valid for any number of mass components, provided the system is only subject to one kinetic constraint $\mathbf{U}^\top \mathbf{p} = \mathbf{m}^\top \mathbf{v} = 0$.

Numerical verification of the equipartition of energy

In the case of the simulated Martini lipid bilayer, the numerical velocity covariance matrix in $\text{nm}^2 \text{ps}^{-2}$ reads, with 2% relative confidence

$$\langle \mathbf{v} \mathbf{v}^\top \rangle = \begin{pmatrix} 7.740 \times 10^{-6} & -3.190 \times 10^{-6} & -3.184 \times 10^{-6} \\ -3.190 \times 10^{-6} & 7.747 \times 10^{-6} & -3.189 \times 10^{-6} \\ -3.184 \times 10^{-6} & -3.189 \times 10^{-6} & 4.461 \times 10^{-6} \end{pmatrix} \quad (9)$$

This compares favorably with the theoretical prediction, using $T = 340\text{K}$, $m_1 = m_2 = 256 \times 14 \times 72 = 258048 \text{ g mol}^{-1}$, $m_3 = m_w = 5140 \times 72 = 368640 \text{ g mol}^{-1}$ and $m_t = 884736 \text{ g mol}^{-1}$, expressed in the same unit as above.

$$k_B T \left[\mathcal{M}^{-1} - \frac{\mathbf{U} \mathbf{U}^\top}{m_t} \right] = \begin{pmatrix} 7.755 \times 10^{-6} & -3.193 \times 10^{-6} & -3.193 \times 10^{-6} \\ -3.192 \times 10^{-6} & 7.755 \times 10^{-6} & -3.193 \times 10^{-6} \\ -3.193 \times 10^{-6} & -3.193 \times 10^{-6} & 4.470 \times 10^{-6} \end{pmatrix} \quad (10)$$

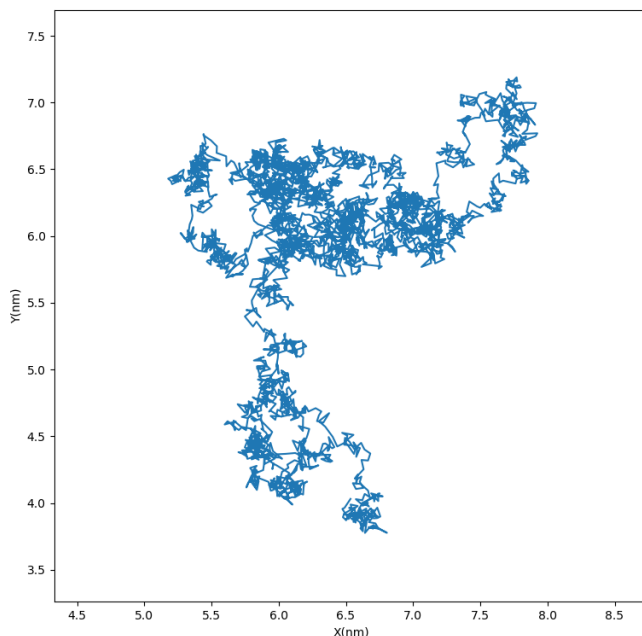


Figure 1: Horizontal projection of the Brownian diffusion of the center of mass of the upper leaflet, every 10 ps, during 400 ns.

Diffusive behavior of the center of mass

Figure 1 represents a sample of Brownian center of mass equilibrium displacement of one leaflet in the x, y plane. Parameterizing the displacement covariance matrix \mathcal{D} as

$$\begin{pmatrix} \langle (\Delta \mathbf{x}_1)^2 \rangle & \langle \Delta \mathbf{x}_1 \Delta \mathbf{x}_2 \rangle & \langle \Delta \mathbf{x}_1 \Delta \mathbf{x}_3 \rangle \\ \langle \Delta \mathbf{x}_2 \Delta \mathbf{x}_1 \rangle & \langle (\Delta \mathbf{x}_2)^2 \rangle & \langle \Delta \mathbf{x}_2 \Delta \mathbf{x}_3 \rangle \\ \langle \Delta \mathbf{x}_3 \Delta \mathbf{x}_1 \rangle & \langle \Delta \mathbf{x}_3 \Delta \mathbf{x}_2 \rangle & \langle (\Delta \mathbf{x}_3)^2 \rangle \end{pmatrix} = 2 \begin{pmatrix} D_1 & D_6 & D_4 \\ D_6 & D_1 & D_4 \\ D_4 & D_4 & D_3 \end{pmatrix} t, \quad (11)$$

Figure 2 shows the asymptotic linear diffusion regime of the mutual quadratic displacements along the x direction. In addition, averaging the relations $\Delta X_1(t)(m\Delta X_1(t) + m\Delta X_2(t) + m_w\Delta X_3(t)) = 0$ and $\Delta X_3(t)(m\Delta X_1(t) + m\Delta X_2(t) + m_w\Delta X_3(t)) = 0$ leads to two additional relations

$$\begin{aligned} m_w D_3 + 2m D_4 &= 0; \\ m(D_1 + D_6) + m_w D_4 &= 0. \end{aligned} \quad (12)$$

One typical numerical simulation gives the following list of values:

Covariant diffusion coefficients ($\mu\text{m}^2\text{s}^{-1}$)	
$D_1 = 4.19 \pm 0.17$	$D_4 = -2.35 \pm 0.13$
$D_2 = 4.11 \pm 0.20$	$D_5 = -2.41 \pm 0.11$
$D_3 = 3.33 \pm 0.10$	$D_6 = -0.75 \pm 0.13$

$$\begin{aligned} 1 + \frac{m}{m_w} \frac{D_4 + D_5}{D_3} &\simeq -8.4 \times 10^{-5}; \\ 1 + \frac{m}{m_w} \frac{(D_1 + D_2 + 2D_6)}{D_4 + D_5} &\simeq -1.1 \times 10^{-4}, \end{aligned} \quad (13)$$

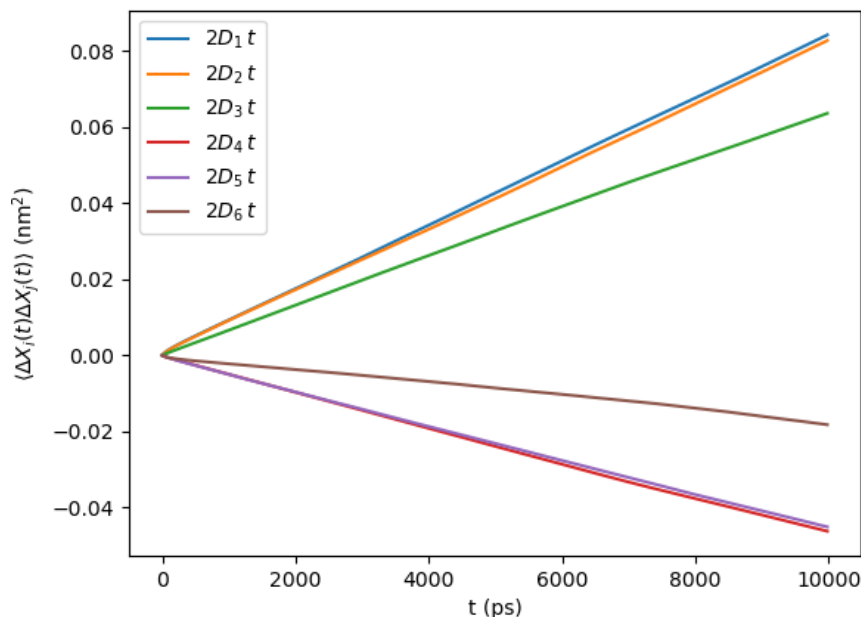


Figure 2: Average displacements correlation matrix $\langle \Delta X_i(t) \Delta X_j(t) \rangle$, averaged over $10 \mu\text{s}$. Diffusion coefficients D_1, \dots, D_6 can be estimated from a linear fit of the second half of the curves (100-200 ps).

confirming the validity of the approach.

Estimation of the confidence interval

The bootstrap method consists in randomly resampling a set of randomly fluctuating data in to estimate their intrinsic variability. It is rigorously established when the fluctuating data are ensured to be statistically independent and gaussian. Otherwise it provides us with a systematic estimate of the sample to sample variability of an average quantity.

Here we have $N_r = 25$ consecutive runs indexed with α at our disposal, which we assume to be essentially weakly correlated (though there are always long lived hydrodynamic fluctuations) [3]. Each run gives a satisfactory estimate of the fitted $D_i^{(\alpha)}$ or friction $b^{(\alpha)}, \eta^{(\alpha)}$ coefficients. 50 synthetic samples are build from the reference $\{\alpha\}$ sample set by drawing at random, and with replacement 25 values. The corresponding average values of the synthetic samples provides us with a variance $\sigma^2(\overline{D}_i)$, $\sigma^2(\overline{b})$, $\sigma^2(\overline{\eta})$ that we take as a basis for our "2 σ " confidence intervals.

References

- [1] Siewert J. Marrink, H. Jelger Risselada, Serge Yefimov, D. Peter Tieleman, and Alex H. de Vries. The martini force field: coarse grained model for biomolecular simulations. *The Journal of Physical Chemistry B*, 111(27):7812–7824, 2007.
- [2] Mark James Abraham, Teemu Murtola, Roland Schulz, Szilárd Páll, Jeremy C. Smith, Berk Hess, and Erik Lindahl. GROMACS: High performance molecular simulations

through multi-level parallelism from laptops to supercomputers. *SoftwareX*, 1-2:19–25, sep 2015.

- [3] William H. Press, Saul A. Teukolsky, William T. Vetterling, and Brian P. Flannery. *Numerical recipes in C*. Cambridge University Press, 1997.